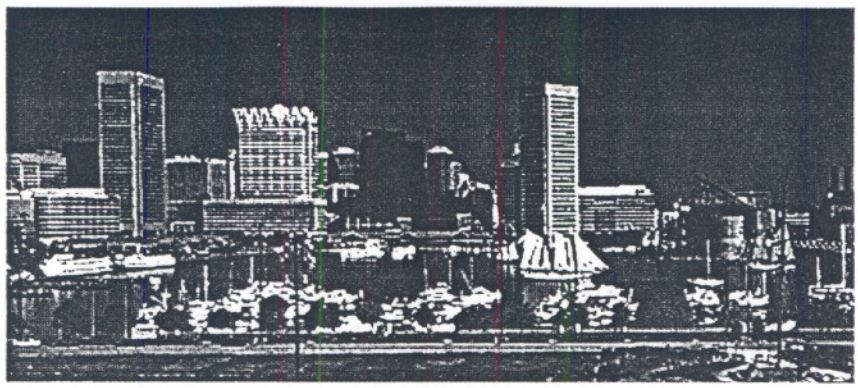

IMTC®/2000

Proceedings of the 17th IEEE Instrumentation and Measurement Technology Conference

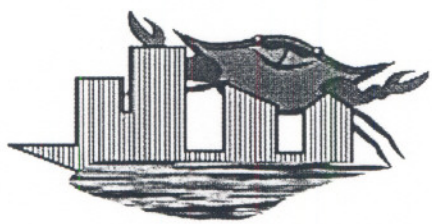

Smart Connectivity: Integrating Measurement and Control

Volume 3

Hilton Hotel and Towers
Baltimore, Maryland, USA – May 1-4, 2000

IMTC/2000 is dedicated to the memory of Joseph F. Keithley

IEEE Catalog Number: 00CH37066 – ISBN: 0-7803-5890-2

Additional copies may be ordered from:

IEEE Service Center
445 Hoes Lane
Piscataway, NJ 08855-1331 USA

IEEE Catalog No. 00CH37066

ISBN 0-7803-5890-2 (softbound edition)
ISBN 0-7803-5891-0 (casebound edition)
ISBN 0-7803-5892-9 (microfiche edition)

ISSN 1091-5281

Printed in the U.S.A.

Non-Iterative Waveform Deconvolution Using Analytic Reconstruction Filters with Time-Domain Weighting

Sandip Roy[1] and Michael Souders[2]
Massachusetts Institute of Technology, Cambridge, MA sandip@mit.edu
[2]National Institute of Standards and Technology, Gaithersburg, MD souders@eeel.nist.gov

Abstract *A new deconvolution approach is described for reconstructing fast step-like or impulsive signals that have been measured with a sampling oscilloscope for which an impulse response estimate is available. The approach uses analytic reconstruction filters to control noise amplification, and a new non-iterative filter optimization that is based on a calculated "indicated error" function that is similar in shape to the true error. The new method aids in reporting uncertainties of the deconvolution results and it permits the use of time-domain weighting to optimize the measurement of different waveform features. The performance of the proposed approach is compared with that of the Error Energy/Regularization approach that is currently popular.*

Introduction

The process of deconvolution is often required to reconstruct a signal from a noisy, filtered representation of it. In our application, a time-domain signal representation is obtained from a sampling oscilloscope, for which an impulse response estimate is available. Often, the bandwidth of the oscilloscope is on the order of, or even less than the equivalent bandwidth of the input signal being measured. Deconvolution is used to remove the effects of the oscilloscope's response, via inverse filtering, in order to obtain a more accurate estimate of the original signal. As discussed by many authors, deconvolution is an ill-posed problem: Measurement noise components in the output signal become highly amplified in the reconstruction of the input signal at frequencies where the oscilloscope response approaches zero [1]. Various filtering approaches are used to control this behavior, but any filter necessarily removes some components of the original signal that is being recovered. Techniques for finding the optimum filter have been the main concern of many deconvolution studies [2-11]. (See [1] and its references for a good overview of the literature.) However, less attention has been given to the optimization criteria that are used and the relationship of these criteria to overall goals, including the estimation and reporting of uncertainties associated with the deconvolution process. Filter optimization in this context is the focus of the work reported here. In particular, we propose (a) the use of analytic filters with "higher order Gaussian" form; and (b) a new non-iterative algorithm to optimize the filter parameters that can be applied in the time domain. The optimization algorithm produces an *indicated error* signal that can be represented in either domain. This signal is similar in shape to the true error, and optimization criteria based on it (e.g., mean-squared error) are minimized at or near the same filter parameters that minimize the true error. The advantages of this method for us are threefold: It permits the use of time-domain weighting functions; the filter can be described analytically for our customers; and it often produces lower errors than competing methods. The use of weighting allows optimization of the errors in selected regions of the waveform. For example, weighting the transition region of step-like signals more heavily permits more accurate transition duration measurements to be made; conversely, weighting non-transition regions more heavily allows aberrations to be estimated more accurately. The use of analytic filter functions aids in reporting the uncertainties of the deconvolution results as will be explained later. For the types of waveforms used in our work, the method (without weighting) generally performs as well as or better than other popular methods such as the error energy regularization method reported in [11]. When weighting is used to optimize a selected region of the waveform, the errors in some cases can be reduced by a factor of two or three.

Background

For a system with impulse response $v(t)$, the output resulting from an input $x(t)$ is given by

$$z(t) = x(t) \circledast v(t) + n_z(t) \qquad (1)$$

where $\circledast$ designates the convolution operator, and $n_z(t)$ is the added measurement noise. In the frequency domain, (1) is represented as

$$Z(\omega) = X(\omega) \bullet V(\omega) + N_z(\omega) \qquad (2)$$

Although $N_Z(\omega)$ is unknown, an estimate of the original input signal can be obtained from a direct deconvolution in the frequency domain given by

$$\hat{X}(\omega) = \frac{Z(\omega)}{\hat{V}(\omega)} = \frac{Z(\omega)}{V(\omega) + N_D(\omega)} \qquad (3)$$

where $N_D(\omega)$ includes any errors in the estimate of $V(\omega)$.

0-7803-5890-2/00/$10.00 © 2000 IEEE

For the work described here, we consider $N_D(\omega)$ to be negligibly small.

Because the noise components of $\hat{X}(\omega)$become large at frequencies where $\hat{V}(\omega)$ is small, the raw deconvolution result given by (3) is usually low-pass filtered so that (3) becomes

$$\hat{X}_F(\omega) = \frac{Z(\omega)}{\hat{V}(\omega)} F(\omega) \qquad (4)$$

where $F(\omega)$ is the filter response [1]. A parametric form is chosen for $F(\omega)$ and the filter is then optimized based on a cost criterion. The filter response given in (5) has frequently been used for $F(\omega)$ [e.g., 3,4,5,11], and filters of this form are called regularization operators:

$$F(\omega) = \frac{\hat{V}(\omega)\,\hat{V}(\omega)^*}{|\hat{V}(\omega)|^2 + \lambda + \gamma |L(\omega)|^2} \qquad (5)$$

where $|\bullet|$ denotes magnitude, superscript * denotes the complex conjugate and $L(\omega)$ is the Fourier transform of the second difference operator (used to control smoothness). Variables γ and λ are the optimization parameters for this filter and often correspond to specific criteria used in the cost function [1]. In [1,11], a cost function based on the estimated error energy has been used effectively.

Deconvolution results based on (4) have two sources of error. First, the choice of the mathematical form of $F(\omega)$ determines the minimum error that can be achieved for a given problem and level of noise, $N_Z(\omega)$. Assuming that the filter parameters can be optimized to achieve the true minimum error, no additional error is accrued. However, since the true error cannot be known directly, the filter parameters must be chosen based on heuristic optimization criteria, and additional errors are created when the optimization fails to minimize the true error.

In the next sections, we discuss a new form for the filter, $F(\omega)$, and a new optimization criterion that can be used to select the filter parameters.

"Measurement bandwidth" and selection of filters

NIST provides measurement services for reference pulse generators that customers in turn use to calibrate other instrumentation. For these services, we not only need to estimate the test signal accurately, but we also need to derive confidence bounds associated with our estimates. Clearly though, if the measurement and deconvolution processes are band limited, we cannot give unqualified bounds for the signal estimate because arbitrarily large signal components could go undetected if their frequencies are sufficiently high. Generally, the prescribed noise filter determines the limiting bandwidth of the signal estimate, assuming that $\hat{v}(t)$ is accurately known.

The plan at NIST is to report the filter used to establish the "measurement bandwidth" that ultimately limits our measurement capability. Then the true signal, $x(t)$, when convolved with the reported noise filter, $f(t)$, will be asserted to lie within stated bounds around the estimated signal, $\hat{x}(t)$, with a given confidence (e.g., 95%). This avoids the dilemma of trying to bound an estimate when there are signal components beyond the bandwidth of the measurement process. However, if the "measurement bandwidth" as determined by the noise filter is significantly greater than either the bandwidth capability of the customer or of the bandwidth of the signal, there is no important information lost. The customer can test this by measuring the signal himself, and low-pass filtering the data record with our noise filter. If the filter has no appreciable effect, then all significant information has been covered by the test report. If the filter does have an appreciable effect, the test report is still valid when applied to the filtered data. Since the noise filter will be reported and possibly implemented by our customers, we prefer simple analytic filters that do not depend on our impulse response estimate, $\hat{v}(t)$. Choosing low-pass filters that are not dependent on the impulse response estimate is most appropriate for applications where the impulse response itself is a low-pass filter. Fortunately, this typifies the response of sampling oscilloscopes.

The computation of the confidence bounds themselves will be the subject of a future paper.

In addition to having an analytic form, the filter should be compact in both the time and frequency domains. Significant ringing in the spectrum, $F(\omega)$, of the noise filter is detrimental to the deconvolution because noisy high frequency components are passed through the filter. In the time domain, the impulse response, $f(t)$, of the filter should also be compact, i.e., limited ringing, to localize its effects. Ideally, $f(t)$, $t > 0$ and $F(\omega)$, $\omega > 0$ are both monotonically decreasing functions assuming symmetric centered responses. As suggested by N. Paulter of NIST, filters of the forms given in (6) and (7) were considered as candidates that could approximate these characteristics, where $m > 1$, and σ_t and σ_f are variables that establish the "widths" in the respective domains. (While these are monotonically

$$f(t) = e^{-0.5\left|\frac{t}{\sigma_t}\right|^m} \qquad (6)$$

$$F(\omega) = e^{-0.5\left|\frac{\omega}{\sigma_f}\right|^m} \qquad (7)$$

decreasing functions for t, $\omega > 0$, their Fourier Transforms are not.) Analytical expressions for the Fourier transforms of these filters can only be determined for $m = 1$ or 2. Based on computer simulations however, $f(t)$, $t > 0$, and $F(\omega)$, $\omega > 0$, are both found to be strictly monotonic only for $1 \le m \le 2$ for either filter. However, all $m \ge 1$ were considered for the filter design since higher power

arguments in exponentials produce sharper time and frequency domain transitions. Values of m greater than 2 produce some ringing in their Fourier transform, but as we will show, in some cases it dies out quickly. The performance of different filters were compared using Gaussian signals for $x(t)$ and $v(t)$, normally distributed noise for $n_2(t)$, and the minimum mean squared error in $\hat{x}(t)$ as the criterion for comparisons. Among filters of the form given in (6), the Gaussian form ($m = 2$) consistently produced the

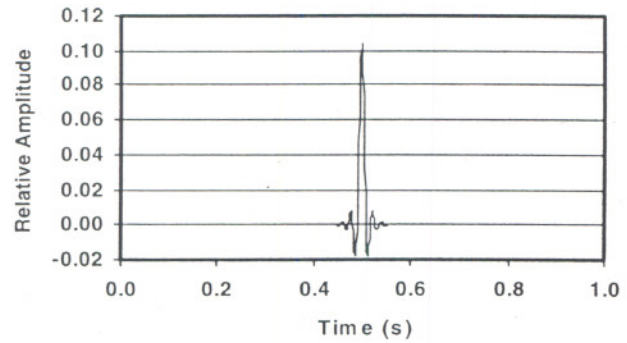

Figure 1. "Higher-order Gaussian" filter, $m = 8$.

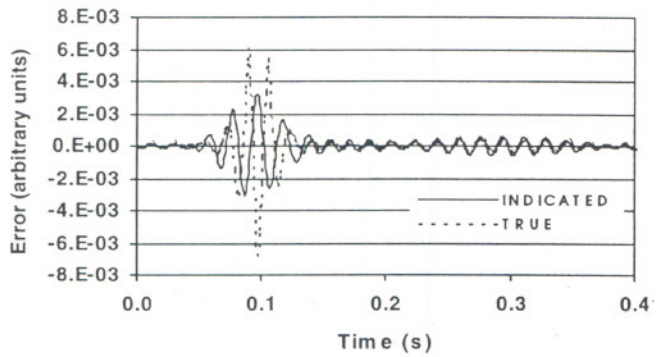

Figure 2. Indicated error (multiplied by 2) and true error.

lowest minimum mean-squared error (varying σ_t). Filters with $m < 2$ did not provide a sufficiently sharp cutoff, while filters with $m > 2$ did not adequately attenuate high frequency noise components because of frequency domain ringing. In contrast, filters of the form given in (7) performed best for $m \geq 2$. The time-domain ringing produced by the higher order filters dies out quickly, and the sharp cutoff afforded by larger values of m allowed the cutoff to be extended to higher frequencies, resulting in less attenuation of the signal components. Figure 1 shows a time-domain (inverse Fourier transform) plot of a filter given in (7) for $m = 8$. Further, the reconstruction errors at optimum σ_f and m were smaller than those produced by the optimum filter of the type given in (6). Based on the comparisons, the filters given by (7) are preferable, where σ_f and m are the two parameters to be optimized. Such filters were also compared to the regularization filter given in (5), where λ and γ were optimized using the minimum error energy criterion [11]. Results are given in a later section.

Optimization

An obvious error criterion is the mean-squared difference between the signal estimate and the true signal, yielding

$$Cost = \frac{1}{N}\sum_{n=0}^{N-1}\left[\hat{x}(n) - x(n)\right]^2. \qquad \textbf{(8)}$$

(When sampled rather than continuous signals are considered, we will use n and k as the respective discrete time and frequency indices). As explained earlier, it would sometimes be desirable to use a weighted error criterion, where a time-domain weighting function is applied to the difference. This gives the modified cost function

$$Cost_W = \frac{\sum_{n=0}^{N-1}\left[w(n)\bullet\left(\hat{x}(n) - x(n)\right)\right]^2}{\sum_{n=0}^{N-1} w(n)}, \qquad \textbf{(9)}$$

where $w(n)$ is the time-domain weighting function. Unfortunately, since $x(n)$ is unknown, neither (8) or (9) can be evaluated directly, and indirect methods and other cost functions must be used, many of which are described in [1]. The various tradeoffs associated with these are also discussed in [1]. Their effectiveness often depends on subjective judgement or heuristic techniques. Others cannot make use of time-domain weighting because phase information is not included in the cost function [11]. We propose a new cost function having the same form as (9), where an *indicated error* $i(n)$ given by (10) substitutes for $\hat{x}(n) - x(n)$:

$$i(n) = ifft\left[\frac{Z(k)}{\hat{V}(k)}F(k)(1-F(k))\right], \qquad \textbf{(10)}$$

where *ifft* [•] indicates the inverse Fourier transform of [•]. This gives the following cost function:

$$Cost_{WI} = \frac{\sum_{n=0}^{N-1}\left[w(n)\bullet i(n)\right]^2}{\sum_{n=0}^{N-1} w(n)}. \qquad \textbf{(11)}$$

Based on observations of simulated data, the function $i(n)$ tends to have a shape similar to that of $\hat{x}(n) - x(n)$, particularly when the optimum filter parameters are approached. An example is shown in fig. 2. Here, the plotted errors are the results of a deconvolution in which the input signal was a unit step-like waveform with the transition centered at t = 0.097 s (see fig. 4). As fig. 2

illustrates, the noise components of the two waveforms are similarly shaped, while the signal components (centered around t = 0.097 s) are approximately 180° out of phase with each other (an explanation is given later in the Additional Remarks and Observations section). Furthermore, the cost given by (11) reaches a minimum at nearly the same filter parameters that minimize the true mean-squared error given by the cost function in (9), as illustrated in fig. 3. In this example, the rms indicated error reaches a minimum at a filter cutoff frequency of 50 Hz, while the true rms error is minimized at a cutoff frequency of 52 Hz. The difference in true error for the two frequencies in this case is only 4.4% of the true minimum error. Plots of indicated and true error versus exponent m (in (7)) show similar results.

Results and examples

Simulations were run using analytical functions for the impulse response, and either analytical or real measured signals for the input waveform. Both step-like and impulsive waveforms were used for the input. The relative bandwidths (-3 dB) of the input and impulse response waveforms were varied, and different amounts of noise were added to the convolution results. Deconvolutions were performed using the proposed (*indicated error*) method as well as the Dabóczi regularization method [11] (based on a minimum error energy criterion) that is currently used in an oscilloscope calibration system [12]. The deconvolution errors for the two methods were compared, and the errors were also compared to the errors that were achieved at the true minimum (i.e., when the filter parameters for either method were adjusted to minimize the true error). Selected results are presented in the following subsections.

When step-like input signals were used with the proposed method, the convolution results were first differentiated using a first difference operator, and the deconvolution was performed in the frequency domain on the Fourier transform of the differentiated signal. The time-domain result of the deconvolution was calculated by integrating the inverse Fourier transform of the frequency domain result with a complementary operator. The filter errors of the two complementary operators compensate each other so no net errors accrue.

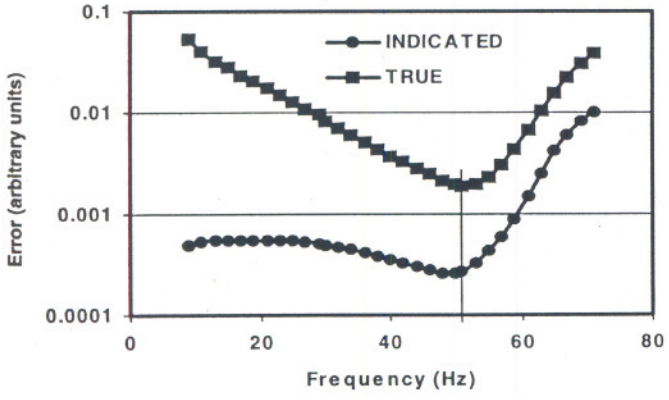

Figure 3. Rms error versus frequency for the true and indicated error functions. (m = 8)

Analytical Signals

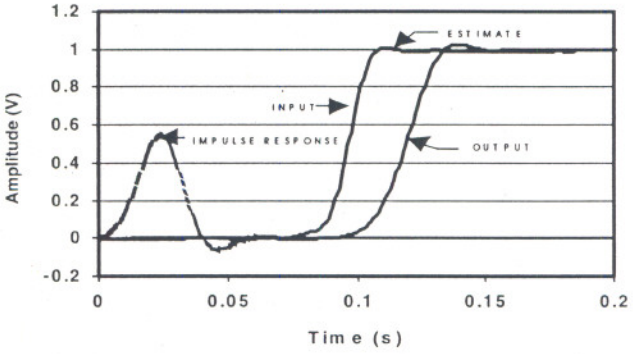

Figure 4. Waveforms, with estimate optimized using transition region weighting. Input and estimate are coincident within plot resolution.

Unit Gaussian step-like input signals (the cumulative density function of a Gaussian distribution) and unit-area Gaussian impulse responses were used with three different bandwidth ratios (bandwidth of the system response to the equivalent bandwidth of the input signal): 2/3, 1, and 3/2. For each of these, Gaussian noise ($\sigma = 2 \times 10^{-4}$) was added to the convolution result, yielding $z(n)$. For several different values of m, σ_f was optimized to minimize the cost function given in (11). The results are presented in Table I. The "Error-in-Error" column reports how far off the found minimum error is from the true minimum error, i.e.,

$$Error\text{-}in\text{-}Error = 100 * \frac{(found\ rms\ error) - (true\ rms\ error)}{(true\ rms\ error)}. \quad (12)$$

For all of the results in Table I, uniform weighting, $w(n)$, was used. Note that in all cases, the *indicated error* optimization found a solution quite close to the true optimal solution, indicating that the optimization method itself adds very little to the overall estimation error.

Real Signals

In other simulations, the input signal was obtained from actual measurements of a step-like signal. The measurement data was first low-pass filtered to minimize residual high frequency noise components added by the measurement system. This filtered input signal, $x(t)$, $0 \le t \le 1$, with an equivalent bandwidth of 23 was convolved with a "rounded second-order" impulse response $v(t)$ with an equivalent bandwidth of 22. By adding noise $n_z(t)$ to the result, the

Table I

BW Ratio	Exponent (m)	True Minimum Error (x 10^{-4})	Error-in-Error (%)
2/3	10	16.7	4.2
1	10	5.08	3.1
3/2	10	2.98	3.7
2/3	7	16.7	3.4
1	7	6.05	0.7
3/2	7	3.45	1.0
2/3	4	28.3	5.9
1	4	9.14	0.0
3/2	4	4.45	0.9

output $z(t)$ was produced. Four different levels (rms value) of noise, $n_z(t)$, ranging from 10 μV to 10 mV per volt of step amplitude were added to the convolution results. The portion of these signals lying between t= 0 and t = 0.2 is plotted in fig. 4 (from t = 0.2 to t = 1, the signal is settling and plots of that region are less revealing). Input signal estimates, $\hat{x}(n)$, were produced using the proposed *indicated error* method as well as Dabóczi's *error energy* regularization method. Filters of the form given in (7) were used with the indicated error method, while the regularization filter in (5) was used with Dabóczi's method. With the former, optimization was performed using uniform weighting ($w_U(t) = 1$ for all t), transition region weighting ($w_T(t) = 1$ in the transition region and $w(t) = 0$ elsewhere), and settling region weighting ($w_S(t) = 1 - w_T(t)$). The comparative results are plotted in fig. 5 as the ratio of the proposed (labeled *new*) deconvolution errors to the Dabóczi error-energy deconvolution errors. The errors were computed using the three different weightings to show how well each method performed in the different regions of the waveform. The weighted error computation is given by

$$\varepsilon_w = \left[\frac{\sum_{n=0}^{N} \left[w(n) \bullet (\hat{x}(n) - x(n)) \right]^2}{\sum_{n=0}^{N} w(n)} \right]^{1/2} \quad . \qquad (13)$$

In the cases where the errors are evaluated in the same region of the waveform that was optimized (those shown in fig. 5), the new method produced errors on the order of (ratio ≈ 1.0) those produced by the *error-energy* method for noise levels of 1 mV and 10 mV, and significantly smaller errors (ratio < 1.0) for lower noise levels. Optimizations of the transition and settling regions were particularly effective. Fig. 6 plots the same errors for the proposed method, under optimized conditions, on an absolute rather than relative scale. Note that the errors in many cases are substantially larger than the level of added noise. This degree of noise amplification is largely due to the relative bandwidths involved, and points out the importance of minimizing the error under such conditions.

Additional remarks and observations

An analytical justification for the efficacy of the *indicated*

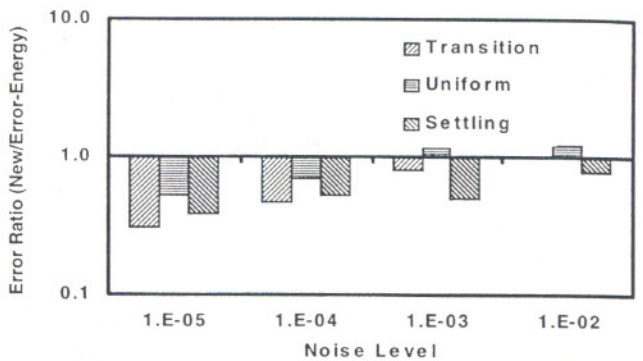

Figure 5. Deconvolution error ratios: (new method) ÷ (error-energy method).

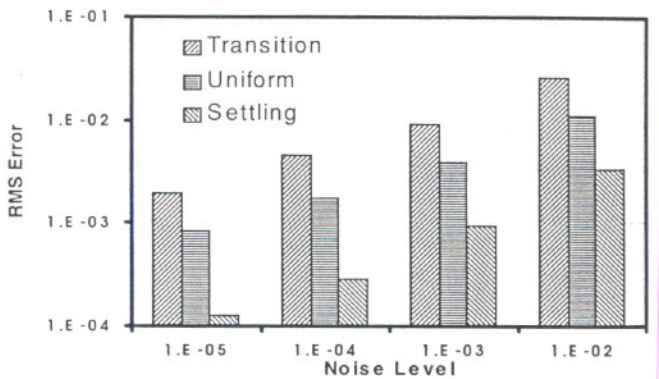

Figure 6. RMS errors from proposed method, at the noise levels given in fig. 5.

error cost function has not been found, although intuitive arguments can be made. First note that the function $Y(\omega) = F(\omega)(1-F(\omega))$ has a band-pass form. In fig. 7, a typical raw deconvolution result, $Z(\omega)/V(\omega)$, is plotted along with $Y(\omega)$, where $F(\omega)$ is nearly optimal. For $Z(\omega)/V(\omega)$, the region before the minimum is dominated by signal components, and the region after the minimum is dominated by amplified noise components. With no time-domain weighting, the optimal filter parameters are found (equivalently) by minimizing the energy in the product of these two frequency-domain functions, and that minimum will occur when the filter - 3 dB frequency equals the frequency at which $Z(\omega)/V(\omega)$ is minimum, and the spectral

"width" of $Y(\omega)$ is minimum, i.e., where m is maximum. In practice, at very large m the found minimum is based on a very small number of spectral lines, causing large variance due to noise. Therefore, m is restricted to values ≤ 14 to provide more spectral averaging. The spectral components of $Z(\omega)/V(\omega)$ that are "sampled" by $Y(\omega)$ are good representations of the deconvolution error. They contain the (significant) noise components that are passed by $F(\omega)$ and therefore included in $\hat{X}(\omega)$, as well as the (significant) components of $X(\omega)$ that are filtered by $F(\omega)$ and thus excluded from $\hat{X}(\omega)$. (Note that these two components are added in the indicated error, while their difference is found in the true error; however, since they are uncorrelated, the energy in both cases is the same.) Of course, as in all deconvolution processes, any component of $X(\omega)$ that is significantly below the amplified noise level will go undetected, which is why it is important to specify the band-limiting filter that is used.

When time-domain weighting is used, the picture is more complicated: The weighting changes the effective frequency content since $[Z(\omega)/V(\omega)][Y(\omega)]$ is convolved with the spectrum of the weighting function. As a result of this smearing and the phase relationships between the *indicated error* function and the weighting, the minimum error in some cases occurs at low values of m (e.g., 2 to 4), particularly when the settling region is selected by the weighting.

There is a false minimum at $f = 0$ in the curve of cost (11) versus σ_f of the noise filter. In practice, this minimum is excluded and the remaining minimum is used in the optimization.

Conclusions

A new deconvolution approach has been developed that uses analytic filters of higher order Gaussian form to control noise amplification while minimizing time-domain ringing. The filter parameters are optimized using a non-iterative method based on an *indicated error* cost function. The *indicated error*, computed from the raw deconvolution and a bandpass filter that is derived from the noise filter, is similar in shape to the true error, and reaches a minimum at nearly the same filter parameters that minimize the true error. Since the indicated error can be represented in the time domain, time-domain weighting can be used to optimize the deconvolution in selected regions of the waveform. For typical step-like waveforms encountered at NIST, the approach performs as well or better than the error energy regularization method that has also been under consideration, and offers the additional advantage that the analytic noise filter can be specified easily and used to clarify the uncertainties associated with the measurement and deconvolution process.

Acknowledgments

J. P. Deyst, N. G. Paulter and G. N. Stenbakken each contributed valuable suggestions during the course of this work. Deyst's experience with applying deconvolution in NIST measurement services was important in focusing the direction of this work. His help in considering analytic filter forms, providing insight into the benefits and shortcomings of existing deconvolution methods, and discussing the results of this research was invaluable. As noted earlier, Paulter suggested the use of the "higher order Gaussian" functions for the noise filter. And Stenbakken helped to clarify the intuitive explanation of the *indicated error* optimization. D. R. Larson is also gratefully acknowledged for performing the comparison deconvolutions using the error energy regularization method reported in fig. 5.

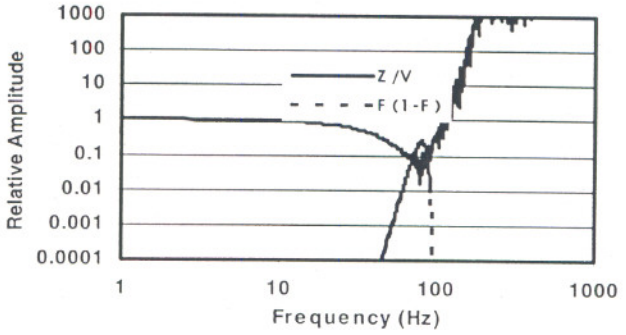

Figure 7. Functions $Z(\omega)/V(\omega)$ and $F(\omega)(1-F(\omega)$.

References

[1] T. Dabóczi, "Deconvolution of transient signals," Ph.D. dissertation, Technical University of Budapest, available as Tech. Rep. Of the Technical University of Budapest, Ser. Elect. Eng., no. TUB-TR-94-EE12, Aug. 1994.

[2] P. B. Crilly, "A quantitative evaluation of various iterative deconvolution algorithms," IEEE Trans. Instrum. Meas., vol. 40.

[3] A. N. Tikhonov and V. Y. Arsenin, "Solutions of Ill-Posed Problems," John Wiley & Sons, Washington, D.C., 1977.

[4] K. Miller, "Least-Squares Method for Ill-Posed Problems with a Prescribed Bound," SIAM J. Math. Anal., vol 1, Feb., 1971.

[5] N. S. Nahman, "Software correction of measured pulse data," in Fast Electrical and Optical Measurements, NATO ASI Series, T. E. Thompson and L. H. Luessen, Eds. Dordrecht, The Netherlands: Nartin Nijhoff, 1986.

[6] B. Parruck and S. M. Riad, "An optimization criterion for iterative deconvolution," IEEE Trans. Instrum. Meas, March 1983.

[7] M. Bertocco, C. Narduzzi, C. Offelli, and D. Petri, "An improved method for iterative identification of bandlimited linear systems," in IEEE Instrumentation and Measurement Technol. Conf., Atlanta, CA, May 14-16, 1991, CH2940-5/91.

[8] N. H. Younan, et. Al., "On correcting HV impulse measurements by means of adaptive filtering and deconvolution," IEEE Trans. Power Delivery, vol. 6, no. 2, 1990.

[9] T. Dhaene, et. al., "Generalized iterative frequency domain deconvolution technique," in IEEE Instrumentation and Measurement Tech. Conf., Irvine, CA, May 1993, 93CH3291-0.

[10] N. G. Paulter, "A causal regularizing deconvolution filter for optimal waveform reconstruction," IEEE Trans. Instrum. Meas., vol. 43, no. 5, Oct. 1994.

[11] T. Dabóczi and I. Kollár, "Multiparameter Optimization of Inverse Filtering Algorithms," IEEE Trans. Instrum. Meas., April. 1996.

[12] J. Deyst, et al., "A Fast Pulse Oscilloscope Calibration System," IEEE Trans. Instrum. Meas., vol. 47, October 1998.